Piotr J. Cywinski | Katia Nchimi Nono | Loïc J. Charbonnière
Tommy Hammann | Hans-Gerd Löhmannsröben

Photophysical evaluation of a new functional terbium complex in FRET-based time-resolved homogenous fluoroassays

Suggested citation referring to the original publication:
Phys. Chem. Chem. Phys. 16 (2014), pp. 6060–6067
DOI http://dx.doi.org/10.1039/C3CP54883J

PCCP

PAPER

View Article Online
View Journal | View Issue

Photophysical evaluation of a new functional terbium complex in FRET-based time-resolved homogenous fluoroassays†

Cite this: *Phys. Chem. Chem. Phys.*, 2014, **16**, 6060

Piotr J. Cywiński,*[ab] Katia Nchimi Nono,[c] Loïc J. Charbonnière,[c] Tommy Hammann[ab] and Hans-Gerd Löhmannsröben[a]

Received 22nd November 2013,
Accepted 10th January 2014

DOI: 10.1039/c3cp54883j

www.rsc.org/pccp

A new functional luminescent lanthanide complex (LLC) has been synthesized with terbium as a central lanthanide ion and biotin as a functional moiety. Unlike in typical lanthanide complexes assembled *via* carboxylic moieties, in the presented complex, four phosphate groups are chelating the central lanthanide ion. This special chemical assembly enhances the complex stability in phosphate buffers conventionally used in biochemistry. The complex synthesis strategy and photophysical properties are described as well as the performance in time-resolved Förster Resonance Energy Transfer (FRET) assays. In those assays, this biotin-LLC transferred energy either to acceptor organic dyes (Cy5 or AF680) labelled on streptavidin or to quantum dots (QD655 or QD705) surface-functionalised with streptavidins. The permanent spatial donor–acceptor proximity is assured through strong and stable biotin–streptavidin binding. The energy transfer is evidenced from the quenching observed in donor emission and from a decrease in donor luminescence decay, both associated with simultaneous increase in acceptor intensity and in the decay time. The dye-based assays are realised in TRIS and in PBS, whereas QD-based systems are studied in borate buffer. The delayed emission analysis allows for quantifying the recognition process and for auto-fluorescence-free detection, which is particularly relevant for application in bioanalysis. In accordance with Förster theory, Förster-radii (R_0) were found to be around 60 Å for organic dyes and around 105 Å for QDs. The FRET efficiency (η) reached 80% and 25% for dye and QD acceptors, respectively. Physical donor–acceptor distances (r) have been determined in the range 45–60 Å for organic dye acceptors, while for acceptor QDs between 120 Å and 145 Å. This newly synthesised biotin-LLC extends the class of highly sensitive analytical tools to be applied in the bioanalytical methods such as time-resolved fluoroimmunoassays (TR-FIA), luminescent imaging and biosensing.

Introduction

Luminescent lanthanide complexes (LLCs) represent a unique class of emitting compounds highly promising for bioanalytical applications. Their potential has already been demonstrated in drug screening assays,[1] luminescent cellular imaging,[2] homogenous[3] and heterogeneous[4] immunoassays, FRET fluoroassays[5] or in bioassays to determine protein concentration.[6] Typically, an LLC contains an organic chelate, central lanthanide ion, and optionally, a molecular spacer terminated with a functional group. The organic chelate acts as an ''antenna'' that first harvests and then transfers light to the central lanthanide ion (Fig. 1). Because of the above chemical assembly, LLCs combine high extinction coefficients provided by the organic antenna[7–9] and well-distinguished emission bands characteristic for the coordinated lanthanide ion. The sharp emission bands originate from the 4f-orbitals, which are effectively shielded by the filled 5s and 5p orbitals. Since those transitions are weakly influenced by the environment, the LLCs produce emission with narrow and well-separated bands with very long decay times (up to several milliseconds). The application of antenna also assists in a large (~150 nm) spectral separation (quasi Stokes shift) that facilitates luminescent signal detection without inner filter effect.

[a] *Department of Physical Chemistry, Institute of Chemistry, University of Potsdam, Karl-Liebknecht-Str. 24-25, 14476 Potsdam-Golm, Germany*
[b] *NanoPolyPhotonics, Fraunhofer Institute for Applied Polymer Research, Geiselberstr. 69, 14476 Potsdam-Golm, Germany. E-mail: piotr.cywinski@iap.fraunhofer.de; Fax: +49 331 568-3000; Tel: +49 331 568-3332*
[c] *Laboratoire d'Ingénierie Moléculaire Appliquée à l'Analyse (LIMAA) IPHC - UMR 7178 - CNRS ECPM, 25 rue Becquerel, 67200 Strasbourg, France*

† Electronic supplementary information (ESI) available. See DOI: 10.1039/c3cp54883j

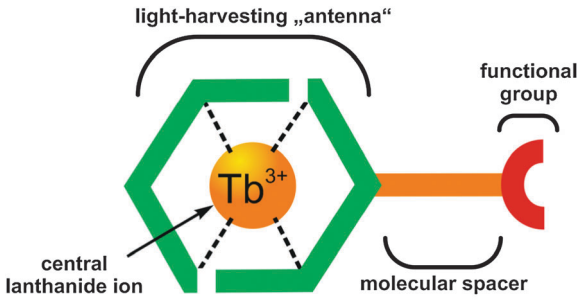

Fig. 1 Modular structure of a luminescent lanthanide complex, here with terbium as a central ion.

In time-resolved LLC-based bioanalytics a significant enhancement in sensitivity can be achieved using an uncomplicated time-gated discrimination between fast-decaying background signals, such as scattering or auto-fluorescence (typically in the nanosecond range) and the micro- or millisecond lanthanide luminescence. Additionally, very narrow LLC emission bands (FWHM ~ 10 nm) allow to discriminate spectrally between the lanthanide luminescence and other signals. Those properties facilitate LLCs' application in multiplexed detection.[5] Another important element is a functional group such as for example NH_2, COOH, NHS, or maleimide. A functional group extends the LLC properties through the ability for being used in bioconjugation. In the LLC structure, the molecular spacer provides complexes with extended flexibility particularly relevant when conjugated with a biomolecule. The spacer assures that the LLC has a minimal influence on the conjugated biomolecule and simultaneously that the LLC photophysical properties stay essentially unaffected.

In recent years, LLC-based Förster Resonance Energy Transfer (FRET) systems have attracted particular scientific attention due to their high sensitivity and excellent performance in immunoassays. FRET is a common technique in the fields of biology, biochemistry, chemistry, medicine and physics. FRET measurements are used in spectroscopy and microscopy to determine distances and conformational changes at the nanometer scale and for highly sensitive, qualitative and quantitative detection of various analytes *in* and *ex vivo*. When using Tb-complexes, the FRET efficiency follows r^{-6} dependence (r being the distance between the energy donor and acceptor)[10] which allows to study inter- and intramolecular interactions in the range of 1 nm to 15 nm and opens new possibilities for studying biomolecular interactions. Noticeably, such an accurate "spectroscopic ruler" can work far below the diffraction limit down to the single molecule level. In FRET systems, the LLCs are commonly combined with organic dyes and less commonly with fluorescent proteins or quantum dots (QDs). QDs are inorganic semiconductor nanocrystals with unique photophysical properties, such as high extinction coefficients (over 1 000 000 M^{-1} cm^{-1} at the excitonic peak) over a broad spectral range and efficient luminescence quantum yield (Φ > 0.7). Noticeably, QDs do not display unfavourable properties such as fluorescence self-quenching and photobleaching.[11] These properties together with the ability to functionalize the QD surface with any biomolecule demonstrate high potential usability of QDs in FRET-based bioanalytical[12,13] and medical applications.[14]

Most often, Eu^{3+} or Tb^{3+} are used as central ions in the LLC-based fluoroassays, mainly due to their strong and well-distinguished emission bands within the visible and near-infrared spectral range. These properties also facilitate uncomplicated luminescence detection with the use of standard spectroscopy and microscopy equipment. Up to date, both Eu^{3+}- and Tb^{3+}-based LLCs have been successfully used in heterogeneous or homogeneous time-resolved fluoroassays to detect biomarkers relevant for pre-clinical research and clinical diagnostics. The Eu^{3+}-based dissociation-enhanced lanthanide fluoroimmunoassay (DELFIA) is one of the first well-known heterogeneous fluoroassays. The ligand used in this assay was built up *via* the combination of diethylene-triamine-pentaacetic acid and sensitizing ligands such as β-diketones.[15] Europium-tris(bipyridine) (Eu-TBP)[16] is another commercialized LLC (Cisbio International) and is being used as a FRET donor in HTRF (homogeneous time-resolved fluorescence) assays and TRACE (time-resolved amplified cryptate emission) technology. Recently, another LLC (Lumi-4, Lumiphore Inc), based on 2-hydroxyisophthalamide ligands,[17] has been successfully introduced as FRET donor in HTRF. Polyaminocarboxylate-based LLC has also been developed recently[18] and found its commercial path to yield the LanthaScreen fluoroassay series. Currently, LLC-based time-resolved FRET assays are used in medical diagnostics, high-throughput screening and lab-on-chip systems.[19] Even though there are numerous literature examples and several commercial applications regarding LLC-based FRET assays, when combined with QDs, the full potential for molecular diagnostics is still to be explored.[20]

Here, in the first part, we report the synthesis route and photophysical properties of a new functional LLC with terbium as a central ion and biotin as a functional group. Then, the complex performance in luminescence FRET assays is presented both with Förster radii and efficiencies. This new biotin-Tb-LLC extends the class of highly sensitive functional lanthanide complexes for application in biochemical and biomedical analysis.

Materials and methods

General methods

Solvents and starting materials were purchased from Sigma-Aldrich, Acros and Alfa Aesar and used without further purification. ^1H and ^{13}C NMR spectra were recorded on Bruker AC 200, Avance 300 and Avance 400 spectrometers operating at 200, 300 and 400 MHz, respectively. Chemical shifts are reported in ppm, with residual protonated solvent as internal reference.[21] IR spectra were recorded on a Perkin Elmer Spectrum One Spectrophotometer and only the most significant absorption bands are given in cm^{-1}.

UV-visible absorption spectra were recorded on a Specord 205 (Analytik Jena) spectrometer. Steady-state luminescence

emission and excitation spectra were recorded on a Horiba Jobin Yvon Fluorolog 3 spectrometer working with a continuous 450 W Xe lamp. Detection was performed with a Hamamatsu R928 photomultiplier. All spectra were corrected for the instrumental response. When necessary, a 399 nm cut off filter was used to eliminate the second order artifacts. Phosphorescence decays were measured on the same instrument working in the phosphorescence mode, with 50 μs delay time and a 100 ms integration window or working in the Time Correlated Single Photon Counting (TCSPC) Lifetime Spectroscopy mode, both using a Xenon flash lamp as the excitation source. Monoexponential decay profiles were fitted with the FAST program from Edinburgh Instruments or with the Data station software from Jobin Yvon. Luminescence quantum yields were measured according to conventional procedures, with optically diluted solutions (optical density < 0.05), using rhodamine 6G in water (Φ = 76.0%)[22] as reference. Estimated errors are ±15%.

Experimental details for FRET measurements

The time-resolved fluoroassays (TR-FA) were carried out on a Kryptor photoluminescence immunoassay reader (Cezanne, Nimes, France). The nitrogen laser (λ_{ex} = 337 nm, PRR = 20 Hz) has been used as an excitation source. The luminescence signals have been collected using two photomultipliers positioned both in the spectral donor ((488 ± 10) nm) and in the acceptor ((665 ± 13) nm for QD655-strep and Cy5-strep and (740 ± 13) nm for QD705-strep and AF680) channel in an 8 ms time window. The TR-FAs were performed at various acceptor concentrations in the range from 0 to 20 nM. The QDs, dyes and biotin-Tb-LLC luminescence were also measured separately to estimate the background signal. The decays were processed using differential correction method (DCM). In all experiments, the biotin-Tb-LLC concentrations have been set to 10 nM.

Results and discussion

Biotin-Tb-LLC as energy donor

Synthesis of the ligand. The biotin-Tb-LLC was obtained from a non-macrocyclic nonadentate ligand biotin-L (Scheme 1). Full experimental details and characterization of the compounds and intermediates can be found in the ESI.†

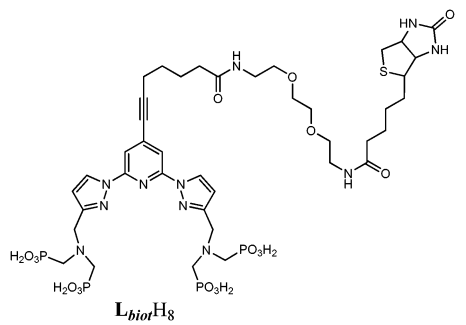

$L_{biot}H_8$

Scheme 1 The chemical structure of the ligand biotin-L used to prepare the final biotin-Tb-LCC.

This ligand contains a highly conjugated pyridine-bispyrazolyl framework as an organic antenna and two amino methyl bis phosphonate moieties to ensure a kinetically and thermodynamically robust coordination to the lanthanide cation.[23,24] The synthetic strategy for the biotin-L preparation is presented in Scheme 2. Substitution of 2,6-bis(3-bromomethylpyrazolyl)-4-bromopyridine **1**[9] with tetraethylaminobis(methanephosphonate)[25] afforded compound **2** in 62% yield. A Sonogashira-type coupling reaction of **2** with 6-heptinoic acid catalyzed by palladium(II) and copper(I) yielded compound **3** with a very good 85% yield.

At this stage, a peptide coupling was carried out with **3** and the amine derivative of biotin **4**[26] using 1-ethyl-3-(3-dimethylaminopropyl)carbodiimide (EDCI) and dimethylaminopyridine as a base, affording the compound **5** with a reasonable 85% yield. Finally, the biotin-L was obtained with a 64% yield after the bromo trimethylsilane-supported phosphoethylic esters' deprotection, methanolysis and the final purification.

Synthesis and characterization of the terbium complex. Biotin-Tb-LCC formation was monitored using UV-Vis absorption and fluorescence spectroscopy. In the titration experiment, $TbCl_3$ solution aliquots were being added to a ligand solution in TRIS/HCl buffer. The absorption and emission spectra were recorded for the different biotin-L–$TbCl_3$ mixtures.

The evolution in the UV-Vis absorption spectra during the titration is presented in Fig. 2. The free ligand spectrum displays two strong absorption bands with maxima at 262 nm and 321 nm, which can be assigned to $n \rightarrow \pi^*$ and $\pi \rightarrow \pi^*$ transitions centered on the pyridyl and pyrazolyl moieties.[27] Upon $TbCl_3$ addition up to one equivalent, both absorption bands undergo a gradual bathochromic shift up to 283 nm and 328 nm, respectively. No further changes were observed for $TbCl_3$ concentrations above 1 : 1 stoichiometry (equimolar mixture).

A change in luminescence emission spectrum during the $TbCl_3$ titration is presented in Fig. 3. The corresponding spectra were recorded from 400 to 650 nm upon excitation at 328 nm, *i.e.* at the ligand absorption band. In the absence of $TbCl_3$, only the ligand-characteristic emission spectrum (below 450 nm) can be observed. Upon addition of up to one $TbCl_3$ equivalent, the ligand fluorescence was disappearing gradually, while sharp emission bands, characteristic for the $^5D_4 \rightarrow {}^7F_j$ ($j = 6 \rightarrow 3$) terbium transitions,[28] were appearing at 485 nm, 545 nm, 580 nm and 620 nm, respectively. The maximum emission amplitude has been reached for an equimolar mixture between the ligand and cation. Further $TbCl_3$ addition resulted in a decrease in the luminescence intensity due to the formation of a binuclear Tb_2-LCC species. In order to confirm the Tb_2-LCC formation during $TbCl_3$ titration above 1 : 1 stoichiometry, the evolving factor analysis was performed for the complete titration data with the SPECFIT software.[29] A bi-component model was fitted to experimental data considering the Tb-LCC and Tb_2-LLC formation. In Fig. 4, the obtained species distribution diagram is showed that allows for an accurate data reconstitution. Considering the marked inflection point, the conditional stability

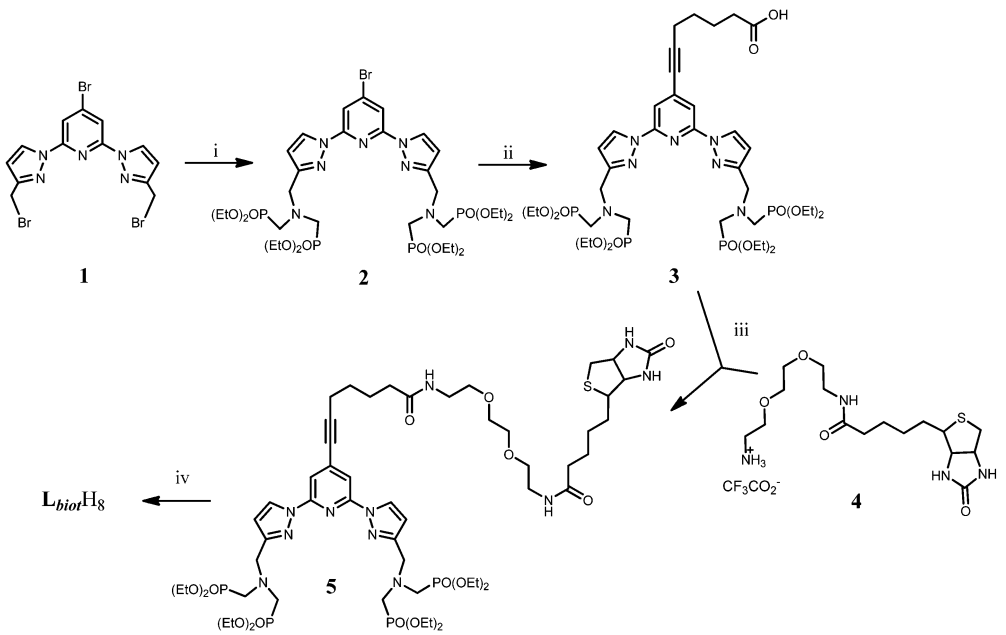

Scheme 2 Synthesis of the biotinylated ligand (biotin-L). (i) $HN(CH_2PO(OEt)_2)_2$, K_2CO_3, CH_3CN, 80 °C, 48 h, 62%. (ii) 6-Heptinoic acid, $[Pd(PPh_3)_2Cl_2]$, CuI, Et_3N, THF, 60 °C, 12 h, 85%. (iii) EDCI, DMAP, DMF, r.t., 4 h, 85%. (iv) TMSBr, 2,6-dimethyl-pyridine, then MeOH, 64%.

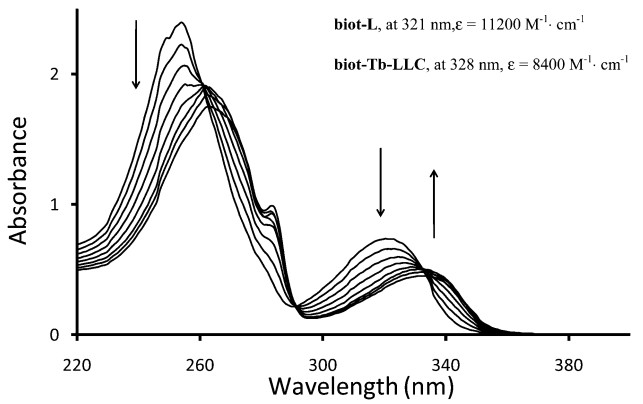

Fig. 2 The evolution in the UV-Vis absorption spectra for a biotin-L solution (concentration c = 5.04 × 10^{-5} M) upon addition of $TbCl_3 \cdot 6H_2O$ aliquots (0.01 M TRIS/HCl buffer, pH 7.4).

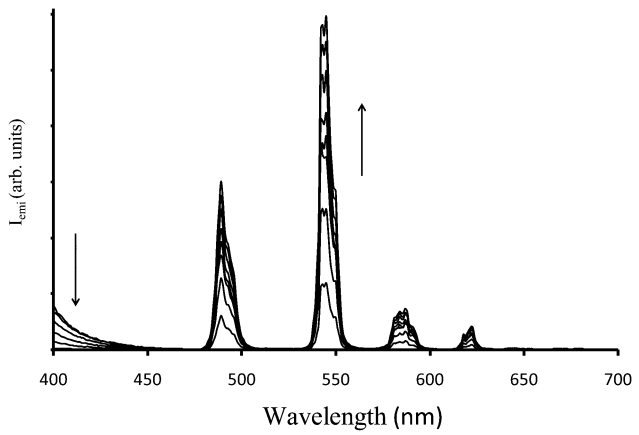

Fig. 3 The evolution in the emission spectra for a biotin-L solution (c = 5.04 × 10^{-5} M) upon addition of $TbCl_3 \cdot 6H_2O$ aliquots (0.01 M TRIS/HCl buffer, pH 7.4, λ_{exc} = 328 nm).

constants for the complex formations could not be determined, which suggests the formation of very stable species.

The biotin-Tb-LLC was prepared by mixing equimolar proportions of biotin-L and $TbCl_3$ in water. After 2 h of equilibration time, the pH was adjusted to pH 7.0 by addition of a diluted NaOH solution. Afterwards, the biotin-Tb-LLC was isolated *via* precipitation and characterized using mass spectrometry and elemental analysis. Finally, the biotin-Tb-LCC was characterized using steady-state and time resolved luminescence spectroscopy. The excited state decay time measured in water was found to be reasonably long (τ_{H_2O} = 2.16 ms). This value indicates a good shielding of the metal by the ligand, preventing non-radiative deactivation processes due to coordination of water molecules in the first cation coordination sphere.[30] This fact was confirmed by the measurement of the luminescence decay time in deuterated water (τ_{H_2O} = 2.92 ms), suggesting a hydration number close to zero.[30] Finally, the luminescence quantum yield (Φ) has been determined giving a value of 0.19. This Φ value has been estimated to be acceptable for FRET experiments.

Organic dyes and quantum dots as energy acceptors. Two kinds of acceptors, namely, organic dyes and QDs have been used in our LLC fluoroassays. In general, organic dyes are less photostable (mainly due to photobleaching) and have lower extinction coefficient than QDs, but dye-based biofunctionalisation is cost-effective and is based on robust and well-established protocols. Moreover, a well-controlled dye-based biofunctionalisation usually retains the biomolecule properties essentially unaffected. In applications, where a long-term

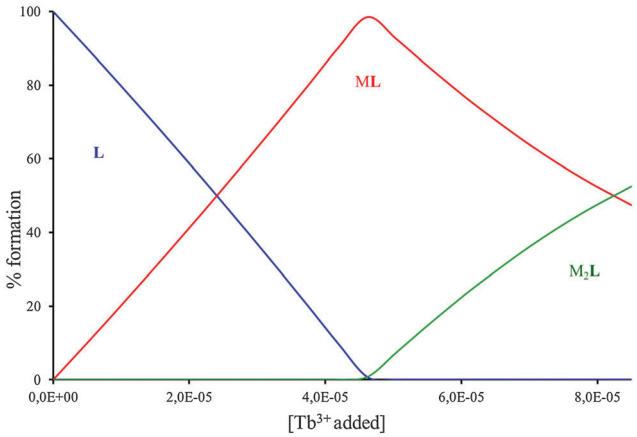

Fig. 4 The evolution in the relative percentages of the species formed during the titration (from luminescence spectroscopy experiments).

photochemical stability is no absolute requirement, organic dyes can be strong competitors for QDs. On the other hand, high extinction coefficients and high quantum yields make QDs promising materials for FRET fluoroassays. In such assays, a crucial issue is the ability to absorb light effectively and transfer energy that finally has an influence on the analytical signal. The size-dependent tuning of the QD emission wavelength is another factor that facilitates the use of quantum dots in multiplexed bioanalysis, which can be complicated with the use of organic dyes. Each acceptor has its own advantages and drawbacks that should be taken into account both in the experimental design and practical product development. In Table 1, the photophysical properties such as absorption maxima, extinction coefficients, fluorescence emission maxima, quantum yields and decay times are presented for all acceptors used in our study. Additionally, Fig. S1 (ESI†) represents the overlapping regions between the emission spectrum of the Tb donor and the different acceptors used in the study.

Biotin-Tb-LLC in homogenous time-resolved fluoroassays. The biotin-Tb-LLC performance was estimated in homogenous fluoroassays with the use of organic dyes and quantum dots as acceptors. In those fluoroassays, the biotin-Tb-LLC transferred energy either to acceptor organic dyes (Cy5 or AF680) labelled on streptavidins or to quantum dots (QD655 or QD705) surface-functionalised with streptavidins. The fluoroassay architectures for both studied systems are presented in Fig. 5. In Fig. 5a, the

Table 1 Absorption maxima (λ_{abs}), fluorescence emission maxima (λ_{em}), extinction coefficients (ε), excited state decay times (τ) in water and luminescence quantum yields (Φ) of acceptors used in this study; the values in brackets denote wavelengths for side maxima in the absorption band

Acceptor	λ_{abs} [nm]	ε [M^{-1} cm^{-1}]	λ_{em} [nm]	Φ [–]	τ [ns]
Cy5	(625), 646	250 000	664	0.28	1.0
Alexa Fluor 680	(620), 679	183 000	702	0.36	1.2
QD655	645[a]	1 100 000[a]	655	0.6	15.2
QD705	680[a]	500 000[a]	705	0.5	20.1

[a] Values at the excitonic peak (taken from the producer's website, www.lifetechnologies.com).

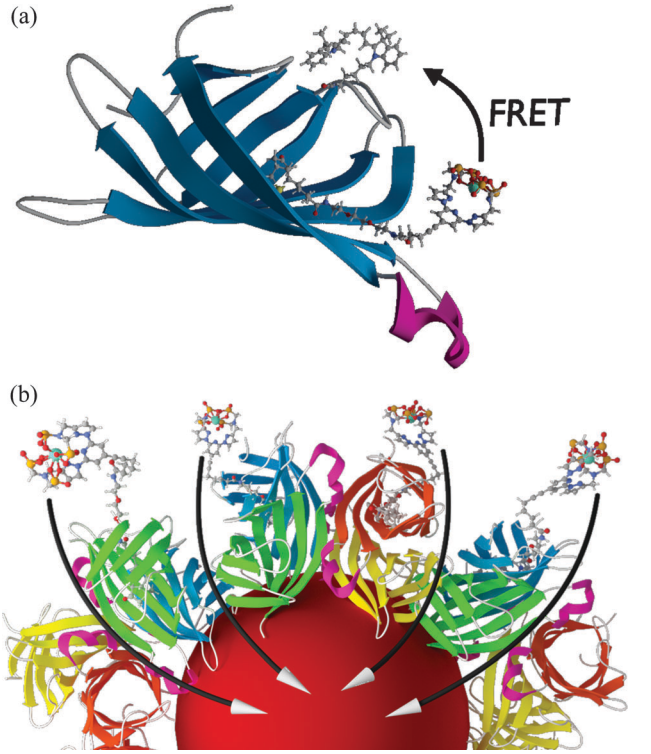

Fig. 5 Two systems studied in this work. Biotin-Tb-LLC (donor) bound (a) to streptavidin monomer labeled with Cy5 and (b) to a streptavidin coated on a quantum dot. The black arrows represent FRET between biotin-Tb-LLC and corresponding acceptors.

biotin-Tb-LLC transfers energy to a Cy5 dye that was bound onto streptavidin, while in Fig. 5b the biotin-Tb-LLC transfers energy to a quantum dot QD655 coated with streptavidins. The permanent spatial donor–acceptor proximity is assured through strong and stable biotin–streptavidin binding. The first-glance architecture assessment gives the impression that the FRET efficiency should be larger for an organic dye, due to shorter distance between donor and acceptor. Nevertheless, due to very high extinction coefficients quantum dots may be superior over organic dyes. In the case of QDs, large light absorptivity can compensate for the large distance between donor and acceptor. The environmental factors such as the presence of particular proteins, ions or pH change can also influence the overall fluoroassay performance. Recently, a very interesting example of a (FRET relay)-based immunoassay has been presented,[31,32] in which FRET first proceeds from a lanthanide complex to QD and then from QD to a dye. The here presented complex can be applied in such systems to improve FRET efficiency and, therefore, sensitivity and robustness for such assay.

In Fig. 6, time-resolved luminescence spectroscopy results are shown for a fluoroassay, in which biotin-Tb-LLCs transfer energy to Cy5 organic dyes. The luminescence decays were collected in PBS for various acceptor concentrations up to 20 nM. The energy transfer has been concluded from the quenching observed in donor emission and from a decrease in donor luminescence decay both accompanied

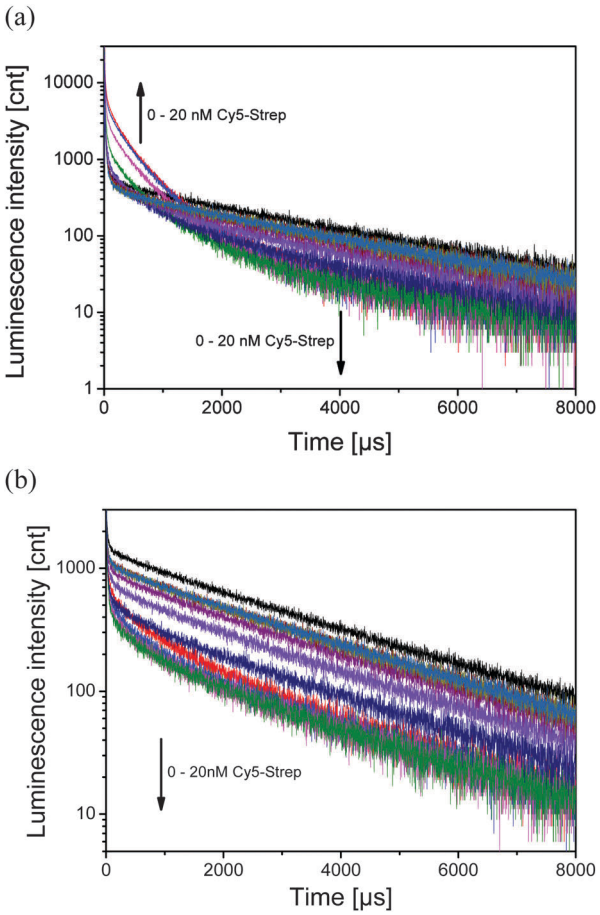

Fig. 6 Time-resolved luminescence spectroscopy results for a fluoroassay, in which biotin-Tb-LLCs transfer energy to Cy5 organic dyes. Luminescence decays were collected in (a) acceptor and (b) donor channel. The sample was excited at 337 nm, the signal was collected through a bandpass filter in the 655 ± 13 nm spectral window. The concentration of the biotin-Tb-LLC was set to 1 μM.

with a simultaneous increase in acceptor intensity and decay time. The decrease is observed since the population of long living LLC decreases, which can be seen as a decrease in intensity as well. The long-decaying contribution in the acceptor channel is due to a crosstalk from the donor emission, usually around 10% of the intensity detected in the donor channel (at 488 ± 10 nm). This effect, however, can be reduced using the differential correction method. In Fig. 6b, in the donor channel one can observe a decrease in luminescence decay associated with gradual quenching in luminescence emission. This effect depicts the depopulation of long living complexes due to the energy transfer to the acceptor.

Differential correction method. The delayed emission analysis allows for quantifying the recognition process and for auto-fluorescence-free detection, which is particularly relevant for application in bioanalysis. In order to support time-gated detection, the Differential Correction Method (DCM) has been successfully used to extract the FRET [$I_{FRET}(t)$] signal from luminescence decays for different acceptor concentrations. Eqn (1) has been applied to determine luminescence intensity coming exclusively from FRET ($I_{FRET}(t)$):

$$I_{FRET}(t) = I_{PAIR,A}(t) - I_{A,A}(t) - \left(\frac{I_{PAIR,D}(t) - I_{A,D}(t)}{I_{Tb,D}(t)}\right) I_{Tb,A}(t) \quad (1)$$

where $I_A(t)$, $I_{Tb}(t)$, and $I_{PAIR}(t)$ are luminescence intensities for acceptor (either dye or QD), biotin-Tb-LLC donor, and combined donor–acceptor pair, respectively. The letters A and D denote whether the signal was collected in the donor or acceptor channel. The DCM has already proven its potential in multiplexed lung cancer assays[33] and protein concentration assays.[6] The method allows enhancing signal-to-background ratio. Therefore, very small changes in FRET signal can be extracted from luminescence decays with improved precision and, consequently, lower LODs can be achieved.

In order to evaluate FRET analytically, the obtained $I_{FRET}(t)$ signals were integrated over the whole time range. The evaluation of the resulting integrals (yielding areas "A") $I_{FRET}(A)$ was done in a time range from 100–1500 μs. The integrated values have been normalized to the minimal value to demonstrate how many times FRET signal increases between initial and saturation values (Fig. 7). In the case of Tb-LCC-to-Cy5 FRET, a 12-fold increase in $I_{FRET}(A)$ was observed. For this system, an LOD equal to 200 pM was determined from a regression of the linear part in Fig. 7.

Based on time-resolved measurements of biotin-Tb-LLC decay times in the absence (τ_D) and in the presence (τ_{DA}) of acceptor, FRET efficiencies calculated from decay time (η_τ) or from intensity (integral from decay in the range 50–1000 μs) (η_I), Förster radii (R_0), and physical distances determined either from decay time (r_τ) or intensity (r_I) evaluation, have been determined for all four studied FRET pairs. The results characterize FRET in all studied pairs (Table 2).

In accordance with Förster theory, Förster radii (R_0) were found to be around 60 Å for organic dyes and around 105 Å for QDs. The FRET efficiency (η) reached 80% and 25% for dye and QD acceptors, respectively. Physical donor–acceptor distances (r) have been determined in the range 45–60 Å for organic dye acceptors, while for acceptor QDs between 120 Å and 145 Å.

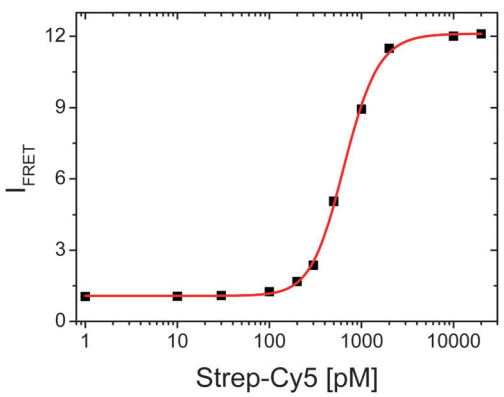

Fig. 7 Cy5-strep titration. In all experiments biotin-Tb-LLC concentration was set to 2 nM. The data points have been fitted with a sigmoid function.

Table 2 Biotin-Tb-LLC decay times in the absence (τ_D) and in the presence (τ_{DA}) of acceptor, FRET efficiencies calculated from decay time (η_τ) and from intensity (integral from decay in the range 50–1000 μs) (η_I), Förster radii (R_0), and physical distances determined either from decay time (r_τ) or intensity (r_I) evaluation

	Biotin-Tb-LLC					
	Cy5-strep		AF680-strep		QD655-strep	QD705-strep
FRET parameter	TRIS	PBS	TRIS	PBS	BB	BB
$\bar{\tau}_D$ [ms]	1.8 ± 0.1	2.4 ± 0.3	1.7 ± 0.1	2.38 ± 0.3	1.28 ± 0.1	1.54 ± 0.1
$\bar{\tau}_{DA}$ [ms]	0.85 ± 0.1	1.08 ± 0.1	0.97 ± 0.1	0.90 ± 0.1	1.1 ± 0.1	1.35 ± 0.1
η_τ [–]	0.53 ± 0.03	0.55 ± 0.02	0.43 ± 0.03	0.64 ± 0.02	0.13 ± 0.04	0.14 ± 0.04
η_1 [–]	0.75 ± 0.05	0.71 ± 0.05	0.70 ± 0.05	0.80 ± 0.05	0.26 ± 0.03	0.25 ± 0.03
R_0 [Å]	60		58		106	110
$r_{\tau,I}$ [Å]	58 ± 5/50 ± 5	58 ± 5/52 ± 5	61 ± 5/50 ± 5	53 ± 5/45 ± 5	145 ± 10/126 ± 10	148 ± 10/132 ± 10

Since the biotin-Tb-LLC was designed to function in phosphate buffers such as phosphate buffer saline (PBS), a decrease in LLC performance may occur when applied in other buffers such as borate buffer (BB). This fact could have an influence on the overall fluoroassay performance. Recently, FRET efficiencies equal to 0.6–0.8 were reported for Tb-LCC-to-QD FRET systems based on commercial Tb complexes.[34] The initial idea behind the design and development of this complex was to improve the complex photophysical stability in PBS, which is, by far, the most often used buffer for fluoroimmunoassays. Typically, lanthanide complexes are very sensitive to environment, particularly to the presence of ions that may be competitive to the chemical groups that form chelating antenna. In addition, the presence of water in the first coordination sphere often reduces photophysical stability of a complex. Even though our biotin-Tb-LLC showed partial instability in TRIS and BB, it has demonstrated that a descent luminescence signal can be measured in those buffers. Noticeably, we observed excellent performance in PBS as it has been assumed in the initial design.

Possible errors in the determination of the donor–acceptor distance (*r*). In the donor channel, each luminescence decay was fitted to a biexponential function that considers existence of two luminescent species, namely unbound free biotin-Tb-LLCs and biotin-Tb-LLCs partly quenched *via* FRET. In the acceptor channel, the luminescence decays were fitted to triexponential functions that consider the existence of three luminescent species, namely biotin-Tb-LLC, a free acceptor and sensitized acceptor. Biotin-Tb-LLC emission has to be considered due to a luminescence crosstalk into the acceptor channel. The luminescence crosstalk has been estimated to be up to 10% of the biotin-Tb-LLC intensity usually collected in the donor channel. The average decay times obtained from corresponding fittings were used to estimate FRET efficiency η_τ. The other factor that may have an influence on FRET efficiency is the integration range. The decay integration (used to calculate η_I) was done over a time range (100–1500 μs), while the decay times were obtained from fitting done over the whole time range. An additional effect can be associated with FRET character, which can originate from dynamic and static interactions. All the above mentioned issues may have an influence on differences between FRET efficiency values calculated either from decay integration or exponential function fitting. Since the physical donor–acceptor distance is dependent on Förster radius and FRET efficiency, the errors from FRET efficiency calculation have an influence on the final *r* value. The difference between donor–acceptor distances calculated either from η_τ or η_I ranged from 10 to 16 percent for dye acceptors and from 10 to 13 percent for QD acceptors. Comparing these differences to experimental errors, one can note larger divergence for dye-based systems, up to three times experimental error, than for QD systems, where the *r* values are slightly above the experimental error.

Conclusions

In this time-resolved FRET study, we demonstrated that our new functional Tb-LLC can be used for highly sensitive biosensing in different types of FRET fluoroassays (with organic dyes and QDs). Simultaneous TR-FRET analysis with the use of different acceptors and different buffers allowed us to perform a very precise characterization of the newly obtained LLC. In conclusion, we have demonstrated the suitability of this new lanthanide complex for fluoroimmunoassays, particularly in phosphate buffers. The complex showed excellent performance in PBS, a very good performance in TRIS and moderate in borate buffer. This newly synthesised biotin-LLC extends the class of highly sensitive analytical tools to be applied in the bioanalytical methods such as time-resolved fluoroimmunoassays (TR-FIA) or luminescent imaging.

Acknowledgements

This research was supported by the Marie Curie European Reintegration Grant QUANTUM$_{DOT}$IMPRINT (PERG05-GA-2009-247825) and the FP7 Collaborative Project NANOGNOSTICS (HEALTH-F5-2009-242264).

References

1 I. Hemmilä and S. Webb, *Drug Discovery Today*, 1997, **2**, 373–381.
2 A. Thibon and V. C. Pierre, *Anal. Bioanal. Chem.*, 2009, **394**, 107–120.
3 H. Mikola, H. Takalo and I. Hemmilä, *Bioconjugate Chem.*, 1995, **6**, 235–241.

4 E. F. Gudgin Dickson, A. Pollak and E. P. Diamandis, *J. Photochem. Photobiol., B*, 1995, **27**, 3–19.
5 D. Geißler, L. J. Charbonnière, R. F. Ziessel, N. G. Butlin, H.-G. Löhmannsröben and N. Hildebrandt, *Angew. Chem., Int. Ed.*, 2010, **49**, 1396–1401.
6 H. Härmä, S. Pihlasalo, P. J. Cywinski, P. Mikkonen, T. Hammann, H.-G. Löhmannsröben and P. Hänninen, *Anal. Chem.*, 2013, **85**, 2921–2926.
7 J. W. Walton, A. Bourdolle, S. J. Butler, M. Soulie, M. Delbianco, B. K. McMahon, R. Pal, H. Puschmann, J. M. Zwier, L. Lamarque, O. Maury, C. Andraud and D. Parker, *Chem. Commun.*, 2013, **49**, 1600–1602.
8 J. Xu, T. M. Corneillie, E. G. Moore, G.-L. Law, N. G. Butlin and K. N. Raymond, *J. Am. Chem. Soc.*, 2011, **133**, 19900–19910.
9 M. Starck, P. Kadjane, E. Bois, B. Darbouret, A. Incamps, R. Ziessel and L. J. Charbonnière, *Chem.–Eur. J.*, 2011, **17**, 9164–9179.
10 L. J. Charbonnière and N. Hildebrandt, *Eur. J. Inorg. Chem.*, 2008, 3231.
11 B. Dubertret, P. Skourides, D. J. Norris, V. Noireaux, A. H. Brivanlou and A. Libchaber, *Science*, 2002, **298**, 1759–1762.
12 W. R. Algar, K. Susumu, J. B. Delehanty and I. L. Medintz, *Anal. Chem.*, 2011, **83**, 8826–8837.
13 E. Petryayeva, W. R. Algar and I. L. Medintz, *Appl. Spectrosc.*, 2013, **67**, 215–252.
14 W. J. Parak, D. Gerion, T. Pellegrino, D. Zanchet, C. Micheel, S. C. Williams, R. Boudreau, M. A. Le Gros, C. A. Larabell and A. P. Alivisatos, *Nanotechnology*, 2003, **14**, R15–R27.
15 E. Soini and I. Hemmilä, *Clin. Chem.*, 1979, **25**, 353–361.
16 H. Bazin, M. Préaudat, E. Trinquet and G. Mathis, *Spectrochim. Acta, Part A*, 2001, **57**, 2197–2211.
17 E. G. Moore, A. P. S. Samuel and K. N. Raymond, *Acc. Chem. Res.*, 2009, **42**, 542–552.
18 P. Ge and P. R. Selvin, *Bioconjugate Chem.*, 2008, **19**, 1105–1111.
19 A. Kupstat, M. U. Kumke and N. Hildebrandt, *Analyst*, 2011, **136**, 1029–1035.
20 N. Hildebrandt, L. J. Charbonnière, M. Beck, R. F. Ziessel and H.-G. Löhmannsröben, *Angew. Chem., Int. Ed.*, 2005, **44**, 7612–7615.
21 H. E. Gottlieb, V. Kotlyar and A. Nudelman, *J. Org. Chem.*, 1997, **62**, 7512–7515.
22 J. Olmsted, *J. Phys. Chem.*, 1979, **83**, 2581–2584.
23 K. Nchimi Nono, A. Lecointre, M. Regueiro-Figueroa, C. Platas-Iglesias and L. J. Charbonnière, *Inorg. Chem.*, 2011, **50**, 1689–1697.
24 S. Abada, A. Lecointre, M. Elhabiri, D. Esteban-Gomez, C. Platas-Iglesias, G. Tallec, M. Mazzanti and L. J. Charbonnière, *Chem. Commun.*, 2012, **48**, 4085–4087.
25 S. Aime, E. Gianolio, D. Corpillo, C. Cavallotti, G. Palmisano, M. Sisti, G. B. Giovenzana and R. Pagliarin, *Helv. Chim. Acta*, 2003, **86**, 615–632.
26 C. Wendeln, S. Rinnen, C. Schulz, T. Kaufmann, H. F. Arlinghaus and B. J. Ravoo, *Chem.–Eur. J.*, 2012, **18**, 5880–5888.
27 M. Mato-Iglesias, T. Rodríguez-Blas, C. Platas-Iglesias, M. Starck, P. Kadjane, R. Ziessel and L. c. Charbonnière, *Inorg. Chem.*, 2009, **48**, 1507–1518.
28 J.-C. G. Bünzli and C. Piguet, *Chem. Soc. Rev.*, 2005, **34**, 1048.
29 H. Gampp, M. Maeder, C. J. Meyer and A. D. Zuberbühler, *Talanta*, 1985, **32**, 95–101.
30 A. Beeby, I. M. Clarkson, R. S. Dickins, S. Faulkner, D. Parker, L. Royle, A. S. de Sousa, J. A. Gareth Williams and M. Woods, *J. Chem. Soc., Perkin Trans. 2*, 1999, 493–504.
31 W. R. Algar, A. P. Malanoski, K. Susumu, M. H. Stewart, N. Hildebrandt and I. L. Medintz, *Anal. Chem.*, 2012, **84**, 10136–10146.
32 W. R. Algar, D. Wegner, A. L. Huston, J. B. Blanco-Canosa, M. H. Stewart, A. Armstrong, P. E. Dawson, N. Hildebrandt and I. L. Medintz, *J. Am. Chem. Soc.*, 2012, **134**, 1876–1891.
33 D. Geißler, S. Stufler, H.-G. Löhmannsröben and N. Hildebrandt, *J. Am. Chem. Soc.*, 2013, **135**, 1102–1109.
34 K. D. Wegner, L. Phung Thi, T. Jennings, E. Oh, V. Jain, S. M. Fairclough, J. M. Smith, E. Giovanelli, N. Lequeux, T. Pons and N. Hildebrandt, *ACS Appl. Mater. Interfaces*, 2013, **5**, 2881–2892.